PB87-166989

Regional Deposition of Inhaled Reactive Gases

(U.S.) Health Effects Research Lab.
Research Triangle Park, NC

Mar 87

U.S. Department of Commerce
National Technical Information Service
NTIS

TECHNICAL REPORT DATA
(Please read Instructions on the reverse before completing)

1. REPORT NO.	2.	3. RECIPIENT'S ACCESSION NO.
EPA/600/D-87/078		PB87-166989/AS

4. TITLE AND SUBTITLE	5. REPORT DATE
Regional Deposition of Inhaled Reactive Gases	March 1987
	6. PERFORMING ORGANIZATION CODE

7. AUTHOR(S)	8. PERFORMING ORGANIZATION REPORT NO.
Fred J. Miller*, John H. Overton*, and Richard C. Graham**	

9. PERFORMING ORGANIZATION NAME AND ADDRESS	10. PROGRAM ELEMENT NO.
Health Effects Research Laboratory, RTP * U.S. Environmental Protection Agency Northrop Services, Inc. ** Environmental Sciences, RTP	11. CONTRACT/GRANT NO.

12. SPONSORING AGENCY NAME AND ADDRESS	13. TYPE OF REPORT AND PERIOD COVERED
Health Effects Research Laboratory, RTP Office of Research and Development U.S. Environmental Protection Agency Research Triangle Park, NC 27711	14. SPONSORING AGENCY CODE EPA/600/11

15. SUPPLEMENTARY NOTES

16. ABSTRACT

A critical concept in inhal[illegible]oxicology involves the determination of dose as the first component for provid[illegible]erspective to judge the applicability of various toxicological results to human exposure conditions. Available experimental data for reactive gases were reviewed, and basic concepts in the formulation of mathematical dosimetry models were discussed. The complexity of factors influencing dose was illustrated as related to rate constant sensitivity, thickness of the protective layer of the lungs, the choice of anatomical model, ventilatory parameters and path distance. Despite the complexities involved, results obtained thus far illustrate the feasibility of making interspecies dosimetric comparisons as an integral step in evaluating the toxicity of inhaled reactive gases, assisting in experimental design, and providing sensitivity studies to determine parameters and processes needing additional research.

17. KEY WORDS AND DOCUMENT ANALYSIS

a. DESCRIPTORS	b. IDENTIFIERS/OPEN ENDED TERMS	c. COSATI Field/Group

18. DISTRIBUTION STATEMENT	19. SECURITY CLASS (This Report)	21. NO. OF PAGES
RELEASE TO PUBLIC	UNCLASSIFIED	39
	20. SECURITY CLASS (This page)	22. PRICE
	UNCLASSIFIED	

EPA Form 2220-1 (Rev. 4-77) PREVIOUS EDITION IS OBSOLETE

PB87-166989

EPA/600/D-87/078
March 1987

REGIONAL DEPOSITION OF INHALED REACTIVE GASES

Frederick J. Miller,[1] John H. Overton,[1] and Richard C. Graham[2]

[1]Health Effects Research Laboratory
U.S. Environmental Protection Agency
Research Triangle Park, NC 27711

[2]Northrop Services, Inc.
Environmental Sciences
P.O. Box 12313
Research Triangle Park, NC 27709

Correspondence should be send to: Frederick J. Miller, Ph.D., Inhalation Toxicology Division (MD 66), U.S. Environmental Protection Agency, Research Triangle Park, NC 27711

HEALTH EFFECTS RESEARCH LABORATORY
OFFICE OF RESEARCH AND DEVELOPMENT
U.S. ENVIRONMENTAL PROTECTION AGENCY
RESEARCH TRIANGLE PARK, NC 27711

NOTICE

This document has been reviewed in accordance with U.S. Environmental Protection Agency policy and approved for publication. Mention of trade names or commercial products does not constitute endorsement or recommendation for use.

INTRODUCTION

The respiratory tract serves as the portal of entry for many environmental pollutants. Since the pollutant is continuously being removed from the inhaled airstream, the airway concentration in the lungs usually declines distally from the trachea. However, at the same time, the liquid lining layer in the tracheobronchial airways that serves to protect the underlying tissue from insult is declining in thickness and may vary in composition. The interaction of these and other factors often produces a pattern of cellular injury that is more distal in the airways. An example of such a case is for ozone (O_3). In rats exposed to ozone, low concentrations cause a chronic epithelial injury in the proximal alveolar region, and the changes occur in a concentration-dependent manner (Barry et al., 1985). Subchronic inhalation of low concentrations of nitrogen dioxide also produces effects in the proximal alveolar region of rats (Chang et al., 1986). In contrast, formaldehyde, a very reactive gas, exhibits its main effects in the upper respiratory tract (Heck et al., 1986). To understand the implications of these kinds of toxicological results for human health, one must be able to relate the effects observed in these studies to comparable exposure conditions that will occur in man. For improved risk assessments, our understanding of the relationship between animal toxicological results and human exposure conditions must be made quantitative.

A way of doing this is by quantitative extrapolation modeling. This involves combining dosimetry and species sensitivity information in order to extrapolate health effects of concern from animals to man. Here, dosimetry refers to estimating the amount of the chemical delivered to or absorbed by specific target sites. However, knowledge of dose alone is not sufficient for extrapolation. One must also determine whether there is equivalency of biological

response if the same dose is delivered to a target site in an animal species and in man. Thus, species sensitivity data are needed to provide the perspective for constructing a damage function which relates the effective delivered dose to the magnitude of the toxicological response observed. And, of course, an adequate health effects data base must exist from which we wish to make extrapolations.

While we are interested in translating an air concentration to some dose in the respiratory tract, differences in anatomy, ventilatory patterns and the physical and chemical properties of the gas combine in a complex fashion to yield dose. If the delivered dose is of sufficient magnitude either from a short-term, high-level exposure or from long-term exposure to lower levels, damage can occur. Depending upon the magnitude of the damage, effects may be seen at the molecular, cellular, tissue, or organ level. Various host defense systems, such as mucociliary function, bacteriocidal and phagocytic activity of alveolar macrophages, etc. can mitigate the damage of inhaled pollutants. Depending upon the length of the exposure and the concentration of the pollutant, repair processes may not be overwhelmed so that recovery occurs. If such is not the case, progression to a disease state can result. Sorting out the differences in these interspecies relationshps is a formidable task for environmental toxicologists. Knowledge of dose is integral to success.

Experimental data on the uptake of reactive gases is limited in nature. This is primarily due to the requirement of using radiolabeling or isotopic ratio mass spectroscopy techniques in order to study the uptake of the compound in specific regions. There are some experimental data available using studies in which the upper respiratory tract airways are isolated. This allows uptake to be determined for either the upper respiratory tract, total respiratory tract

or lower respiratory tract by differencing or by direct measurement methods. An example for ozone of the kind of data obtained is indicated in Table 1.

As improved methods become available for use in experimental determination of the regional absorption of inhaled reactive gases, data can be obtained which will be useful in validating predictions of theoretical dosimetry models. However, experimental data alone cannot provide the necessary information for examining interspecies differences in dose. There are many exposure scenarios for which it is not practical to obtain experimental data, and thus the focus of this chapter will be on mathematical modeling of the regional absorption of inhaled reactive gases. However, one must keep in mind that the ultimate use of experimental or theoretical absorption data is to allow concentration response curves to be converted to dose response curves for the purposes of intra- and interspecies comparisons of toxicological results.

MODELING THE ABSORPTION OF REACTIVE GASES

Mathematical dosimetry models can be used to estimate exposure levels that produce the same dose in different animals of the same or different species for use in comparing toxicological responses. Models provide an integration of our knowledge and can be used to test concepts and to advance our understanding of toxicological events. The major factors affecting the absorption or uptake of gases in the respiratory tract of man and animals are the morphology of the respiratory tract, the route, depth and rate of breathing, physical chemical properties of the reactive gas, the physical and chemical processes which govern gas transport in the lung, and the physicochemical properties of the lining fluids and tissue material of the airways and gas exchange units. For a discussion of considerations useful in modeling respiratory tract transport and

absorption of reactive gases the reader is referred to Overton (1984), Miller et al. (1985), and Overton, et al. (1987a).

Model Formulation

Mathematical models have been developed that to varying degrees incorporate the above factors. In Table 2, a limited summary of models, the models are classified according to the region of the respiratory tract examined, the gas studied and the species. For a detailed discussion of the formulations of these various models, the reader is referred to the original articles. Here, we briefly describe the major features of the more complex mathematical descriptions.

The change with time in the average cross-sectional concentration in a given airway is related to convection, axial dispersion, and wall losses due to chemical reactions and physical absorption. In addition, more complex models include an expansion/contraction factor to account for the fact the airway dimensions are changing during the breathing cycle. Flux of the gas to the liquid lining of the airways is described in terms of a mass transfer coefficient and the gas phase and liquid phase interfacial concentrations. The liquid lining is comprised of a mucous lined fluid in the conducting airways and a surfactant lined fluid in the gas exchange airways. When the models include both tissue and blood compartments, the mass transfer coefficient depends on the physical and chemical properties of these compartments as well as those of the liquid lining. Figure 1 gives an example of the mathematical formulation for an O_3 dosimetry model.

In order to model chemical reactions and mass transport in the compartments, various input data are needed. Information is needed on the chemical composition of the compartment and on the concentration of the components such as the concentrations of unsaturated fatty acids, free amino acids, sulfhydryl groups,

carbohydrates, etc. The stoichiometry of the reactions of the pollutant with these constituents must also be identified. In the absence of definitive chemical kinetic data, model predictions have been obtained by assuming only physical absorption in the liquid lining or assuming instantaneous irreversible reaction, or both. Model formulations may also include the production of biochemical constituents within compartments. The diffusion coefficient of the gas in a compartment, as well as the Henry's Law constant and partition coefficients relating the interfacial concentrations of the gas, must also be included in the model formulation. Figure 1 summarizes many of the processes modeled and the parameters required to characterize the processes.

The conceptualizations involved in formulating the lower respiratory tract O_3 dosimetry model of Miller et al. (1985) are illustrated in Figure 2. The tracheobronchial (TB) region (Figure 2, panel a), involving the trachea and the branchings from the major bronchi down to the terminal bronchioles, follow various branching patterns in man and animals. These branchings are conceptualized as a series of right circular cylinders which are used to form pathways models for the purposes of mathematical dosimetry modeling. In the TB region, the airways are lined by mucous and the epithelium consists of various cells including Clara cells, goblet cells, and brush cells (Figure 2, panel c). The cilia of the ciliated cells are bathed in the pericilliary fluid and propel the mucus towards the trachea. Two basic concepts exist as to the extent to which mucus covers the pericilliary liquid. Some studies (Luchtel 1978; Kaliner, 1984) indicate that mucus forms a continuous blanket, whereas other studies (Van As, 1977; Jeffrey and Reid, 1977) view the mucous layer as not being continuous. In either case, the variations in thickness value for mucus, even within the

same airway generation, indicate that information on the thickness distribution is of considerable importance in modeling the uptake of reactive gases, since reactions in this layer serve to lessen the insult to underlying tissue. The thinnest non-alveolar tissue is greater than about 7 μm (Barry et al., 1983) and, according to Miller et al. (1985), less than 0.1% of a reactive gas such as O_3 should penetrate beyond a tissue thickness of 2.2 μm. Consideration of these factors leads to a model formulation for ozone that includes air, liquid lining and tissue compartments in the TB region (Figure 2, panel e).

In the pulmonary or gas exchange regions, the airways start to develop alveolar outpocketings and continue to branch into a series of alveolar ducts terminating with alveolar sacs (Figure 2, panel a). This region of the lung is lined with a thin fluid whose chemical constituents may have little effect on the absorption of gases such as O_3 or NO_2. Type I and Type 2 alveolar cells are the main cell types in this region. These cells, along with the interstitial and endothelium tissue, give rise to the capillary network (Figure 2, panel b). Since the air to blood harmonic mean thickness is less than 1μm (Gerr et al., 1978), penetration of the gas to the blood cannot be neglected. Thus, in the pulmonary region, the main compartments of the model formulation include air, liquid lining, tissue and blood as diagrammed in Figure 2, panel d.

Modeling Results

In the following sections, examples of modeling results using various anatomical, ventilatory, and model parameters will be presented. While modeling results are primarily available for ozone, similar studies could be conducted for other reactive gases, such as phosgene and nitrogen dioxide.

Rate Constant Sensitivity Studies - The uptake of O_3 in the human lung due to different liquid lining rate constants has been examined by Miller et al. (1985). While the total percent uptake was found to be essentially independent of the TB liquid lining rate constant for values ranging from 0 up to 10 times the reference rate constant, the distribution of the mass of absorbed O_3 in the different compartments and regions was very different and highly dependent upon the rate constant. In general, the larger the TB liquid lining rate constant, the more absorbed by the TB region and less by the pulmonary region. Also, the increase in rate constant value reduces the penetration of O_3 to the TB tissue. On the other hand, when the pulmonary liquid lining rate constants are varied over comparable limits, essentially the same pulmonary uptake is still observed indicating that chemical reactions in this layer may not play an important role in protecting the underlying pulmonary tissue (Miller et al., 1985).

Effect of the Thickness of the Protective Layer - The thickness of the protective layer can be shown to be critical to the determination of tissue dose (Miller et al., 1985). The thickness of the mucous and surfactant layers has been examined in a number of animal studies (Luchtel 1976, 1978; Yoneda 1976; Adler et al., 1973; Clements and Tierney, 1965; Pattle 1967). There is a considerable range in the estimates of thickness for the various generations in the TB region and in values for the surfactant layer. Also, protective layer thicknesses have not been systematically examined in man. The sensitivity of dose to the thickness of the mucous layer is illustrated in Figure 3 for the human lung. While the thickness being used in the mathematical model does not affect the net dose of ozone, there is a substantial effect on the dose of ozone predicted to penetrate to the underlying tissue in the TB region. When the thickness is varied from 1/2 to twice the reference value, the resulting

change in dose approaches two orders of magnitude in some portions of the TB tree. The differences in tissue dose become less in the latter portions of the TB region due to the gradual decrease of thickness to a common value in the pulmonary region. Variations in the thickness of the mucous layer have little impact on the predicted dose changes in the gas exchange regions of the lung. With respect to surfactant lined regions, decreasing the thickness of this layer can have a marked effect on the resulting tissue dose. Since there are alveolar outpocketings in the respiratory bronchiolar region, it is possible that the liquid lining thickness of the alveoli and in the walls are different. This could result in the uptake of the pollutant being different in these two portions even in the same generation of the lungs.

Effect of Anatomical Models - In order to study the absorption of reactive gases for a given species, information is needed on the number of airways, as well as their lengths, diameters and radii. Such information is usually obtained from replica cast studies. The data obtained is often used to construct anatomical models (e.g., Kliment, 1973; Schreider and Hutchins, 1980; Yeh et al., 1979). The choice of anatomical model may affect the predictions arising from mathematical dosimetry models as illustrated in Figure 4. Simulated net and tissue dose profiles for the guinea pig and rat are illustrated for the various anatomical models studied. Although ventilatory parameters vary widely for the different simulations in view of differences in body weight and other parameters reported by the investigators (for full discussion see Overton et al., 1987a), the simulation curves qualitatively illustrate similarities and differences in predicted dose resulting from the four anatomical models. As with the dose curves predicted for man, the tissue dose is relatively low in

the trachea and increases distally to a maximum around the first pulmonary airway and then decreases rapidly. Proceeding from the trachea, net dose decreases distally throughout most of the TB region; net and tissue dose are essentially the same in the gas exchange regions. While results using the Klement zone models for these two animals species are very similar with respect to the predicted distribution of ozone in the lungs, the computer simulations of dose for the Schreider and Hutchins (1980) guinea pig and the Yeh et al. (1979) rat models demonstrate that significant differences exist in the absorption patterns of these two animals. For example, with the Schreider and Hutchins (1980) guinea pig, there was a much greater difference between the net tracheal dose and the net dose of the first alveolated airway. For the rat, the net dose to the trachea is less than the net dose of the first alveolated generation. The Schreider and Hutchins (1980) and the Yeh et al. (1979) rat models exhibit an increase in dose at the first non-mucous lined or the first alveolated order of the lung model, similar to the increase that is observed in the human lung model simulations. Since the first alveolated region of the lung is where the primary effects of ozone have been observed, it will be important to determine which of these discussed anatomical models are more appropriate for dose estimation in order that the analyses that are combined with tissue sensitivity data can give an accurate extrapolation.

Even for the same species, anatomical models based upon individual paths can be used to assess the variation in the regional delivered dose of inhaled gases on a lobar basis. In Figure 5 are plotted simulation results for the ozone tissue dose of the first alveolated duct as a function of the distance from the trachea to the duct within a given lobe for the anatomical model of Yeh et al. (1979). The right apical lobe receives a greater delivered dose of ozone compared to the other lobes. Two sets of ventilatory parameters were

studied. Although the minute volume was kept the same for both analyses, the simulated tissue dose was 35-57% higher for the lower breath per minute simulation compared to the larger. The rapid shallow breathing of the rat at higher breaths per minute imparts a predicted significant decrease in the ozone dose to the first alveolated duct and could be used as a compensatory mechanism to minimize the penetration of ozone to more sensitive distal regions of the lung. Since the lobe model path lengths are averages, the variations in individual path lengths are probably greater than in anatomical lobe models. Thus, centriacinar tissue doses in an individual animal may vary more than predicted, making it necessary to use anatomical data for actual individual paths to quantitate the variability and damage to this region.

Effect of Ventilatory Parameters - Since ventilatory parameters (tidal volume and breathing frequency) can have a large effect on uptake; an examination of the role of these parameters is of interest. Figures 6A through 6C present the results of an investigation into the effects of ventilatory parameters on the percent uptake in the LRT of rats (using the Yeh et al., 1979 anatomical for a 330 gram rat). The three panels illustrate one way of displaying simulation results than can be useful in helping to better understand the effects of parameter changes on the uptake and distribution of absorbed O_3 in the LRT. Holding $\dot{V}_E$ (193 ml/min) constant and allowing the breathing frequency (breaths per minute) to vary from 80 to 190, the total uptake decreases from 72% to 37% (Figure 6, Panel A). There is a comparable fall off in the pulmonary tissue uptake. The percent uptake by the TB region is essentially independent of breathing frequency for a given minute volume and is approximately 12%. When

tidal volume is held constant (1.84 ml) and breathing frequency varied between 60 and 190 breaths per minute (Figure 6, panel B), the total uptake decreases from 70 to 61% while the pulmonary tissue uptake increases from 49% to 52%. If breathing frequency is held constant at 105 breaths per minute and the tidal volume allowed to vary between 1 and 2.4 mls (Figure 6, panel C), the total uptake increases from 45% to 71%. More strikingly, however, the pulmonary tissue uptake more than doubles, increasing from 27% to 59%. The results in Figure 6 demonstrate that the total and pulmonary tissue percent uptake are more sensitive to changes in tidal volume than to changes in breathing frequency.

Humans increase both tidal volume and breathing frequency upon increased ventilatory demand; the effects of exercise on airway and alveolar tissue dose for normal respiration levels up to those measured on heavy exercise are shown in Figure 7. Note the lack of the effect of exercise on tissue dose for the first generations of the TB airways; however, beyond generation 14, there is a pronounced increase in tissue dose with increasing exercise levels. There is a shift distally in the location of the maximum tissue dose as the exercise levels increase from rest to heavy exercise. The ventilatory parameters for the heavy exercise curve, depicted in Figure 7, correspond to those from the McDonnell et al. 1983 study in which they examined the effects of exercise for ozone concentrations ranging from the current standard of .12 ppm up to .4 ppm. The total quantity of ozone absorbed with the heaviest exercise simulation represents a tenfold increase over that of normal respiration. The vast amount of the increase is related to the increases of uptake in the pulmonary region; the TB region mass increase only by a factor of approximately 1.4.

The changes due to exercise that are illustrated in Figure 7 can be examined by considering the percent uptake by region and compartment (Table 3). Presumably, the major increase in total percent uptake is a result of increases in the pulmonary region due to the decrease in transit time through the tracheobronchial regions and the increase in volume of air moved to the pulmonary or gas exchange units as a result of the increased demand for oxygen during exercise.

An Interspecies Dosimetric Comparison - Figure 8 is an example of an interspecies comparison of net and tissue dose patterns. Plotted are the predicted net and tissue doses versus generation for man (dashed line; the Weibel, 1963, anatomical model) and rat (solid line, the Yeh et al., 1979, anatomical model). To help examine the dose patterns, the first generation of respiratory bronchioles in man has been matched with the first alveolated airway in the rat lung. The junction between the TB conducting airways and the pulmonary region (i.e., in the vicinity of the terminal bronchioles and first pulmonary airway) is where the histopathological data show the first and the most pronounced lesions in O_3 toxicological studies using rats. In both rat and man the predicted maximal dose occurs at or near the junction. Approximately a 6-fold increase in absorption or removal of O_3 is predicted in the first pulmonary airway of the rat compared to man according to the dose curves, which are standardized to a unit tracheal O_3 value. However, nasopharyngeal removal of O_3 in man and rat must be considered to make a more definitive interspecies dosimetric comparison at this point. Nasopharyngeal removal studies are currently being conducted, and when available, will facilitate translation of the net and tissue dose curves into delivered dose curves associated with exposure to O_3.

SUMMARY

A critical concept in inhalation toxicology involves the determination of dose as the first component for providing a perspective to judge the applicability of various toxicological results to human exposure conditions. Available experimental data for reactive gases were reviewed, and basic concepts in the formulation of mathematical dosimetry models were discussed. The complexity of factors influencing dose was illustrated as related to rate constant sensitivity, thickness of the protective layer of the lungs, the choice of anatomical model, ventilatory parameters, and path distance. Despite the complexities involved, results obtained thus far illustrate the feasibility of making interspecies dosimetric comparisons as an integral step in evaluating the toxicity of inhaled reactive gases, assisting in experimental design, and providing sensitivity studies to determine parameters and processes needing additional research.

REFERENCES

Adler, K.B., Wooten, O., and Dulfano, J.M. 1973. Mammalian respiratory mucociliary clearance. Arch. Environ. Health 27:364-369.

Aharonson, E.F., Menkes, H., Gurtner, G., Swift, D.L., and Proctor, D.F. 1974. Effect of respiratory airflow rate on removal of soluble vapors by the nose. J. Appl. Physiol. 27:654-657.

Barry, B. E., Miller, F. J., and Crapo, J. D. 1985. Effects of inhalation of 0.12 and 0.25 parts per million ozone on the proximal alveolar region of juvenile and adult rats. Lab. Invest. 53(6):692-704.

Chang, J.C.F., Gross, E.A., Swenberg, J.A., and Barrow, C.S. 1983. Nasal cavity deposition, histopathology, and cell proliferation after single or repeated formaldehyde exposure in B6C3F1 mice and F-344 rats. Toxicol. Appl. Pharmacol. 68:161-176.

Chang, L., Graham, J. A., Miller, F. J., Ospital, J. J. and Crapo, J. D. 1986. Effects of subchronic inhalation of low concentrations of nitrogen dioxide. I. The proximal alveolar region of juvenile and adult rats. Toxicol. Appl. Pharmacol. 83:46-61.

Clements, J.A. and Tierney, D.F. 1965. Alveolar instability associated with altered surface tension. In: Handbook of Physiology. Section 3, Respiration (W.D. Fenn and H. Rahn, eds.). Vol. II, Chapter 69, pp. 15-84, American Physiological Society, Washington, DC.

Gehr, P., Bachofen, M., and Weibel, E.R. 1978. The normal human lung: ultrastructure and morphometric estimation of diffusion capacity. Respir. Physiol. 32:121-140.

Gerrity, T.R., Weaver, R.A., Berntsen, J.H. and O'Neil, J.J. 1986. Nasopharyngeal and lung removal of ozone during tidal breathing in man. Physiologist 29(4):173.

Heck, H, d'A., Casanova, M., McNulty, M.J., and Lam, C. 1986. Mechanisms of nasal toxicity induced by formaldehyde and acrolein. In: Toxicology of the Nasal Passages. (C.S. Barrow, ed.), pp. 235-247, Hemisphere, Washington.

Jeffery, P.K. and Reid, L.E. 1977. The respiratory mucous membrane. In: Respiratory Defense Mechanism, Part I. (J.D. Brain, D.F. Proctor, and L.M. Reid, eds.), pp. 193-245, Marcel Dekker, Inc., New York.

Kaliner, M., Marom, Z., Patow, C., and Shelhamer, J. 1984. Human respiratory mucus. J. Allergy Clin. Immunol. 73(3):318-323.

Kliment, V. 1973. Similarity and dimensional analysis, evaluation of aerosol deposition in the lungs of laboratory animals and man. Folia Morphol. 21:59-64.

La Belle, C.W., Long, J.E., Christofano, E.E. 1955. Synergistic effects of aerosols. Particulates as carriers of toxic vapors. A.M.A. Arch. Ind. Health 11:297-304.

Luchtel, D.L. 1976. Ultrastructural observations on the mucous layer in pulmonary airways. ICCB Abstract No. 1048. J. Cell. Biol. 70. 350a.

Luchtel, D.L. 1978. The mucus layer of the trachea and major bronchi in the rat. Scan. Elec. Micros. 11:1089-1098.

McDonnell, W.F., Horstman, D.H., Hazucha, M.J., Seal, E., Jr., Haak, E.D., and Salaam, S. 1983. Pulmonary effects of ozone exposure during exercise: dose-response characteristics. J. Appl. Physiol. 54:1345-1352.

McJilton, C., Thielke, J., Frank, R. 1972. Ozone uptake model for the respiratory system. In: Abstracts of Technical Papers. American Industrial Hygiene Conference, May 14-19, 1972, paper no. 45.

Miller, F.J., Menzel, D.B., and Coffin, D.L. 1978. Similarity between man and laboratory animals in regional pulmonary deposition of ozone. Environ. Res. 17:84-101.

Miller, F.J., McNeal, C.A., Kirtz, J.M., Gardner, D.E., Coffin, D.L., Menzel, D.B. 1979. Nasopharyngeal removal of ozone in rabbits and guinea pigs. Toxicol. 14:273-281.

Miller, F.J., Overton, J.H., Meyers, E.T., and Graham, J.A. 1982. Pulmonary dosimetry of nitrogen dioxide in animals and man. In: Air Pollution by Nitrogen Dioxide. (T. Schneider and L. Grant, eds.) Proceedings of U.S.-Dutch International Symposium on NO_X, Maastricht, Netherlands. pp. 377-386, Elsevier Press.

Miller, F.J., Overton, J.H., Jr., Jaskot, R.H., Menzel, D.B. 1985. A model of the regional uptake of gaseous pollutants in the lung. I. The sensitivity of the uptake of ozone in the human lung to lower respiratory tract secretions and exercise. Toxicol. Appl. Pharmacol. 79:11-27.

Miller, F.J., Overton, J.H., Jr., Smolko, E.D., Graham, R.C. and Menzel, D.B. 1987. Hazard assessment using an integrated physiologically-based dosimetry modeling approach: ozone. National Academy of Sciences (in press).

Mockros, L.F., Grotberg, J.B., and Sheth, B.V. 1985. Absorption of noxious gases in pulmonary airways. Abstract, 38th ACEMB Meeting. Chicago, IL, Sept. 30-Oct. 2.

Morgan, M.S., Frank, R. 1977. Uptake of pollutant gases by the respiratory system. In: Respiratory Defense Mechanisms. Part I. (J.D. Brain, D.F. Proctor, and L.M. Reid, eds.), pp. 157-189, Marcel Dekker, Inc., NY.

National Research Council. 1977. Committee on medical and biologic effects of environmental pollutants, subcommittee on ozone and other photochemical oxidants. Toxicology, ozone and other photochemicl oxidants. pp. 323-387, Washington, DC, National Academy of Sciences.

Overton, J.H. 1984. Physicochemical processes and the formulation of dosimetry models. J. Toxicol. Environ. Health 13(2-3):273-294.

Overton, J.H., Graham, R.C., and Miller, F.J. 1987a. A model of the regional uptake of gaseous pollutants in the lung. II. The sensitivity of ozone uptake in laboratory animal lungs to anatomical and ventilatory parameters. Toxicol. Appl. Pharmacol. (in press).

Overton, J.H., Graham, R.C. and Miller, F.J. 1987b. Mathematical modeling of ozone absorption in the lower respiratory tract. National Academy of Sciences (in press).

Pattle, R.E. 1967. Lung surfactant and its possible reaction to air pollution. Arch. Environ. Health 14:70-76.

Schreider, J.P. and Hutchens, J.O. 1980. Morphology of the guinea pig respiratory tract. The Anatomical Record 196:313-321.

Van As, A. 1977. Pulmonary airway clearance mechanisms: a reappraisal. Am. Rev. Respir. Dis. 115:721-726.

Weibel, E.R. 1963. Morphometry of the human lung. 151 pp. Academic Press, New York.

Wiester, M.J., Williams, T.B., King, M.E., Ménache, M.G., and Miller, F.J. 1987. Ozone uptake in awake Sprague Dawley rats. Toxicol. Appl. Pharmacol. (in press).

Yeh, H.C., Schum, G.M., and Duggan, M.T. 1979. Anatomic models of the tracheobronchial and pulmonary region of the rat. Anat. Rec. 195:483-492.

Yokoyama, E., Frank, R. 1972. Respiratory uptake of ozone in dogs. Arch. Environ. Health 25:132-138.

Yoneda, K. 1976. Mucuos blanket of rat bronchus. Am. Rev. Respir. Dis. 114:837-842.

TABLE 1

Ozone Uptake Experiments

Region	Animal	Comments	Reference
URT	Dog	% uptake decreased with flow rate and with increasing O_3 concentration. Mouth breathing removed less O_3 than nose breathing. 37% - 72% uptake depending on condition. (Unidirectional flow; 0.26 - 0.34 and 0.78 - 0.80 ppm)	Yokoyama and Frank (1972)
URT	Rabbit, Guinea Pig	~50% uptake (unidirectional flow). Tracheal and ambient [O_3] linearly related (only one flow rate for each animal used; 0.1 - 2.0 ppm)	Miller *et al.* (1979)
URT	Man	Levels of O_3:0.1, 0.2, 0.4 ppm. Modes of breathing: oro-nasal, nasal, mouth. Breathing frequencies: 12 and 24 BPM. Average uptake ranged from 40 to 48%, depending on mode of breathing and breathing rate but not on O_3 level.	Gerrity *et al.* (1986)
LRT	Dog	Mechanically ventilated dogs. 80% to 87% uptake with two concentration ranges and two ventilatory rates. (0.3 $\pm$ .1 and .77 $\pm$ 0.07 ppm)	Yokoyama and Frank (1972)
LRT	Man	Levels of O_3: 0.1, 0.2, 0.4 ppm. Modes of breathing: oro-nasal, nasal, mouth. Breathing frequencies: 12 and 24 BPM. Average uptake ranged from 89 to 93%, with a small dependence on O_3 level and breathing frequency, but no significant dependence on breathing mode.	Gerrity *et al.* (1986)
TOTAL	Rat	In headout pressure plethysmographs; exposed one hour, % uptake = 41.3 $\pm$ 10.7 SD, 39.4 $\pm$ 7.4 SD, and 42.5 $\pm$ 13.5 SD of inhaled O_3 for 0.3, 0.6, and 1.0 ppm, respectively; no time effects.	Wiester *et al.* (1987)

TABLE 2

DOSIMETRY MODELS

Region Modeled	Pollutant	Animal	Reference	Comments
URT	Many, including O_2, O_3, SO_2, NH_4, HCHO	Rat	LaBelle et al. (1955) NRC (1977)	Based on the concepts of scrubbing tower and distillation equipment design. Model does not account for chemical reactions in mucus or lung tissue.
URT	HCHO	Rat	Chang et al. (1983)	Used to calculate a "dose" for correlations with observed nasal toxicity.
URT	Acetone, O_3, Ether, SO_2	Dog	Aharonson et al. (1974)	Unidirectional steady state flow model with wall loss rate proportional to pollutant concentration.
LRT	O_3, SO_2	Man	McJilton et al. (1972); NRC (1977); Morgan and Frank (1977)	Approximated convection and diffusion in the 24 generation anatomical model of Weibel (1963). No chemical reactions in the liquid lining; tissue assumed an infinite sink for pollutant.
LRT	O_3, NO_2	Man, Rat, Rabbit	Miller et al. (1978, 1982)	Accounted for convection and dispersion in the airways of anatomical models of man and laboratory animals and for diffusion and chemical reactions (instantaneous reaction regime) in the liquid lining; tissue an infinite sink for O_3.

TABLE 2 (Continued)

DOSIMETRY MODELS

Region Modeled	Pollutant	Animal	Reference	Comments
LRT	O_3	Man, Rat, Guinea Pig	Miller et al. (1985) Overton et al. (1987a)	Airway transport is similar to Miller et al. (1978). Takes into account transport and chemical reactions in the liquid lining, tissue, and blood compartments. Reaction rate is proportional to $[O_3]$ in the compartments.
LRT	O_3	Man, Rabbit	Mockros et al. (1985)	Accounts for convection and diffusion in the gas phase. Instantaneous and second order reaction processes are considered in the liquid lining.

TABLE 3

SIMULATED EFFECT OF EXERCISE ON REGIONAL AND COMPARTMENTAL UPTAKE OF O_3 IN MAN[1,2]

Tidal Volume (l)	Breathing Frequency (Breaths per Minute)	Minute Ventilation (l/min)	Total Uptake (%)	Tracheobronchial Region Uptake (%)		Pulmonary Region Uptake[3] (%)	
				Liquid Lining	Tissue	Tissue	Blood
0.5	15	7.5	89.2	18.4	8.3	60.3	2.0
1.0	15	15.0	95.8	10.8	5.2	77.1	2.6
1.75	20.3	35.5	98.5	5.0	2.5	87.9	3.0
2.25	30.0	67.5	99.4	2.8	1.4	92.0	3.1

[1]Table based on Overton et al. (1987b).

[2]Uptake is based on the quantity of O_3 inhaled at the trachea.

[3]The liquid lining absorbs less than 0.3%.

FIGURE 1: Al illustration of equations used to describe the transport and chemical reactions of O_3 in the compartments of the respiratory tract. In the liquid lining, tissue and blood compartments steady state molecular diffusion and chemical reactions are used to describe and approximate the important processes involved in the absorption of O_3. In the air compartment a time-dependent axial dispersion equation is used to approximate the equation of continuity with wall losses and changes in dimensions due to breathing. Definition of terms includes: t = time; x = distance along airway path; z = distance within compartments; $\bar{C}$ = average cross sectional O_3 concentration in the air compartment or lumen; C_c = pointwise O_3 concentration in compartment (subscript c stands for either, liquid lining, tissue, or blood compartments); D = effective dispersion coefficient of O_3 in lumen; D_c = molecular diffusion coefficient of O_3 in a compartment; u = average air velocity in lumen; S = surface area; V = volume of airway; $\dot{V}$ = time rate of change of airway volume; J_w = radial flux to wall; k_g = gas phase mass transfer coefficient; k_{2c} = effective second order chemical rate constants; $[HCl]_c$ = concentration of components that react with O_3; H = Henry's Law constant; C_{li} = liquid layer O_3 concentration at the liquid-air interface. (From Overton et al., 1987b.)

FIGURE 2: The relationships between morphologies and their model representations. Panel a is a schematic of the branching airways of the TB and pulmonary region of man (Panel a based on Weibel, 1963). The generations are labeled from the right, beginning with the trachea. BR, BL and TBL indicate bronchi, bronchioles and terminal bronchioles, respectively; the respiratory bronchioles, alveolar ducts, and alveolar sacs are indicated by RBL, AD and AS, respectively. Below the TB portion of the lung schematic are three cylindrical figures that indicate the model representation of the airways. Panel c shows a diagram of the structure

of the liquid lining and tissue of the TB region (Panel C based on Jeffery and Reid, 1977). The different cells represented are basal (BC), ciliated (CC), brush (BrC), goblet (GC), and nonciliated serous (NCC). Panel e illustrates the model representation of TB liquid lining and tissue compartments. On the left side of the figure, Panel b, is an electron micrograph of the interalveolar septa (Panel b based on Gehr et al., 1978). The air spaces (A), capillaries (C), type I cells and their nuclei (EP1 and NEP1), endothelial cells and their nuclei (EN and NEN), and interstitial space (IN) are indicated. Panel d illustrates the model representation of the liquid lining, tissue and capillaries of the pulmonary region. (From Miller et al., 1987.)

FIGURE 3: The effect of liquid compartment thickness schemes on O_3 tissue dose (curves A, B and C) and on the corresponding net dose (A', B' and C'). Curves A and A': reference curves, thickness scheme A. Curves B and B': thickness scheme B (one-half thickness of scheme A). Curves C and C': thickness scheme C (twice thickness of scheme A). TB = tracheobronchial region (mucous lined); P = pulmonary region (surfactant lined). Multiply figure values by tracheal concentration ($\mu g/m^3$) to obtain dose ($\mu g/cm^2$ per breath). (From Miller et al., 1985.)

FIGURE 4: An illustration of the effect of four different lower respiratory tract anatomical models on predicted net and tissue O_3 dose profiles of guinea pig and rat. Dose is the quantity of O_3 reacting with biological constituents per unit surface area of a zone, order or generation, per unit time per tracheal O_3 concentration. Net dose is the sum of the liquid lining, tissue and blood compartment doses. The source of the anatomical model used is given at the top of each graph. V_T = tidal volume (ml); f = breaths per minute; TB = tracheobronchial region; P = pulmonary region. (Based on Overton et al., 1987a.)

FIGURE 5: The effect of path distance on the tissue dose of the first alveolated generation. The anatomical models used are the rat lobe models of Yeh et al (1979). Path distance is the distance at FRC. Curve A: V_T = 2.4 ml, f = 81 BPM; Curve B: V_T = 1.25 ml, f = 154 BPM. (curves eye fit) (Reprinted from Overton et al., 1987a.)

FIGURE 6: Effect of ventilatory parameters on regional uptake in the rat (Yeh et al., 1979, anatomical model). A. Regional uptake as a function of breathing frequency with $\dot{V}_E$ = 193 ml/min. B. Regional uptake as a function of breathing frequency with V_T = 1.84 ml. C. Regional uptake as a function of tidal volume with breathing frequency = 105 breaths per minute.

FIGURE 7: The effect of exercise on predicted O_3 tissue dose in the lower respiratory tract of man (based on Miller et al., 1985). The level of exercise and its corresponding tissue dose curve are indicated on the figure. V_T = tidal volume (liters); f = breaths per minute; $\dot{V}_E$ = minute volume; TB = tracheobronchial region; P = pulmonary region. (Reprinted from Miller et al., 1987.)

FIGURE 8: An example of a way of comparing species doses by plots of airway dose versus generation for two species, man (dashed curves) and rat (solid curves). The first generations of the pulmonary regions (17 and 16 in the anatomical models for man and rat, respectively) have been matched at the dotted vertical line to allow a better comparison of equivalent regions; this results in the break in the rat generations along the abscissa. The tidal volume (V_T)

FIGURE 5: The effect of path distance on the tissue dose of the first alveolated generation. The anatomical models used are the rat lobe models of Yeh et al (1979). Path distance is the distance at FRC. Curve A: V_T = 2.4 ml, f = 81 BPM; Curve B: V_T = 1.25 ml, f = 154 BPM. (curves eye fit) (Reprinted from Overton et al., 1987a.)

FIGURE 6: Effect of ventilatory parameters on regional uptake in the rat (Yeh et al., 1979, anatomical model). A. Regional uptake as a function of breathing frequency with $\dot{V}_E$ = 193 ml/min. B. Regional uptake as a function of breathing frequency with V_T = 1.84 ml. C. Regional uptake as a function of tidal volume with breathing frequency = 105 breaths per minute.

FIGURE 7: The effect of exercise on predicted O_3 tissue dose in the lower respiratory tract of man (based on Miller et al., 1985). The level of exercise and its corresponding tissue dose curve are indicated on the figure. V_T = tidal volume (liters); f = breaths per minute; $\dot{V}_E$ = minute volume; TB = tracheobronchial region; P = pulmonary region. (Reprinted from Miller et al., 1987.)

FIGURE 8: An example of a way of comparing species doses by plots of airway dose versus generation for two species, man (dashed curves) and rat (solid curves). The first generations of the pulmonary regions (17 and 16 in the anatomical models for man and rat, respectively) have been matched at the dotted vertical line to allow a better comparison of equivalent regions; this results in the break in the rat generations along the abscissa. The tidal volume (V_T)

and breathing frequency (f) are given on the figure. Tissue dose is the predicted dose of the epithelial layer in the tracheobronchial region and of the air-blood barrier in the pulmonary region. Net dose is the total absorbed by the liquid lining, tissue, and blood compartments. (Reprinted from Miller et al., 1987.)

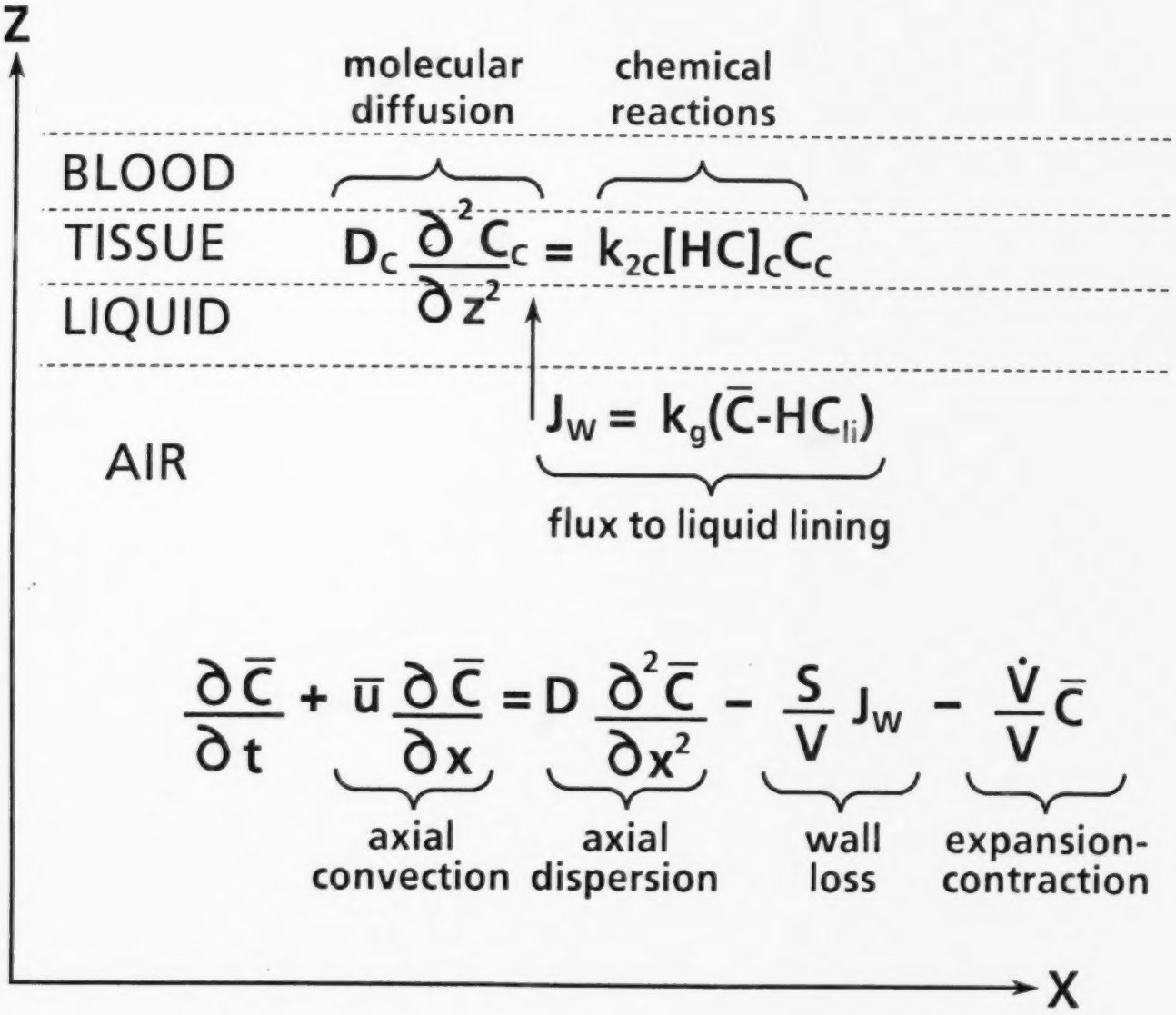
Z
molecular diffusion
chemical reactions
BLOOD
TISSUE
LIQUID
AIR
$D_C \frac{\partial^2 C_C}{\partial z^2} = k_{2C}[HC]_C C_C$
$J_W = k_g(\bar{C} - HC_{li})$
flux to liquid lining
$\frac{\partial \bar{C}}{\partial t} + \bar{u}\frac{\partial \bar{C}}{\partial x} = D\frac{\partial^2 \bar{C}}{\partial x^2} - \frac{S}{V}J_W - \frac{\dot{V}}{V}\bar{C}$
axial convection
axial dispersion
wall loss
expansion-contraction
X

Fig. 1

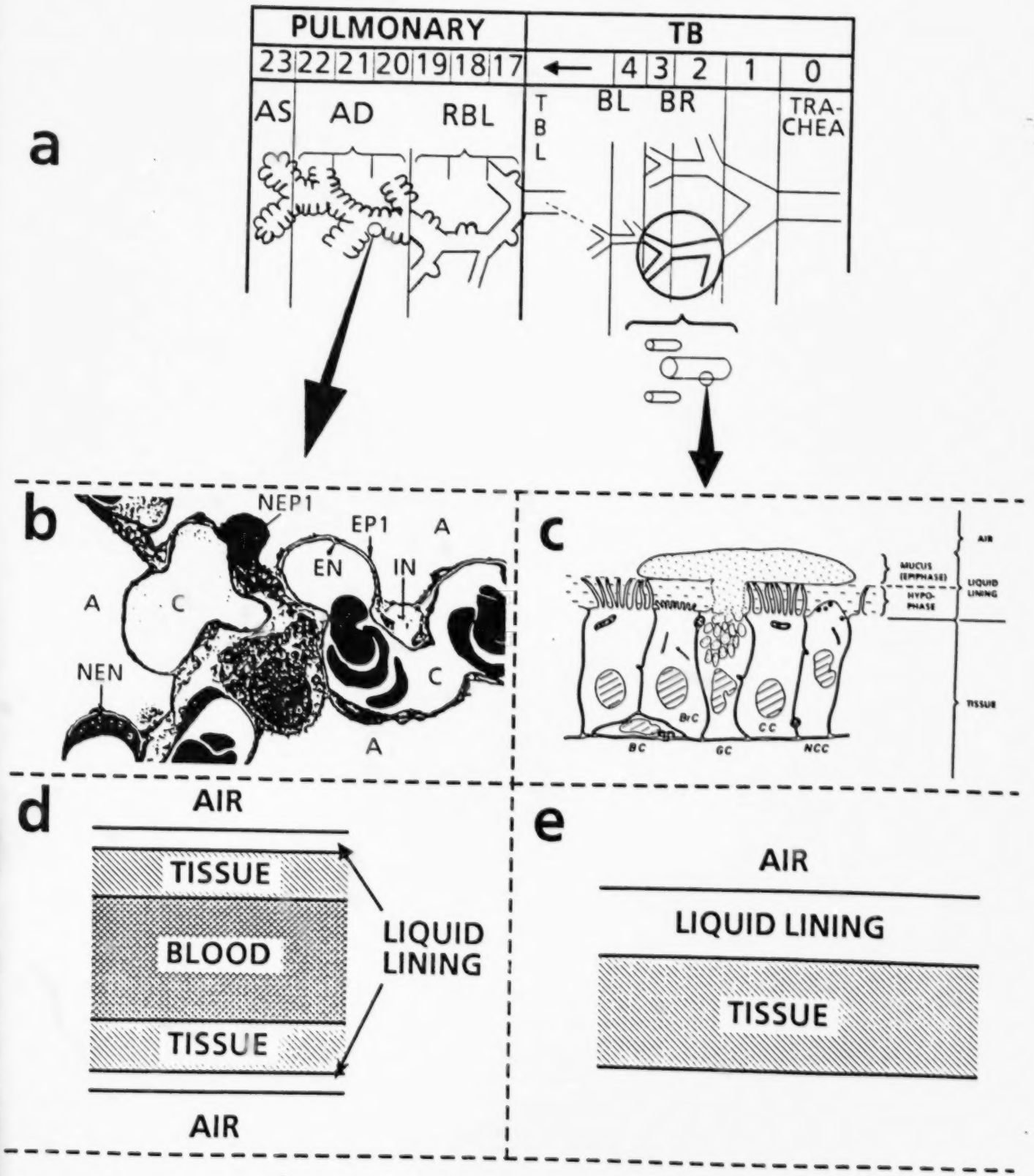
a
PULMONARY
23 22 21 20 19 18 17
TB
4 3 2 1 0
AS
AD
RBL
TBL
BL
BR
TRA-
CHEA
b
NEP1
EP1
A
EN
IN
A
C
NEN
C
A
c
AIR
MUCUS (EPIPHASE)
HYPO-PHASE
LIQUID LINING
TISSUE
BrC
CC
BC
GC
NCC
d
AIR
TISSUE
BLOOD
TISSUE
LIQUID LINING
AIR
e
AIR
LIQUID LINING
TISSUE

Fig. 2

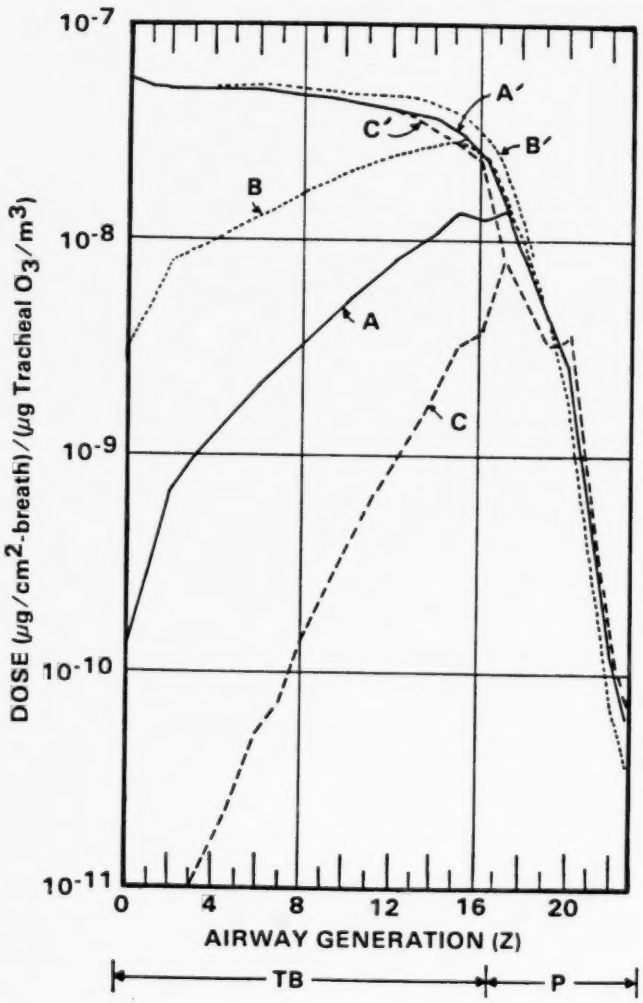
10-7
10-8
10-9
10-10
10-11
DOSE (μg/cm2-breath)/(μg Tracheal O3/m3)
A′
C′
B′
B
A
C
0
4
8
12
16
20
AIRWAY GENERATION (Z)
TB
P

Fig. 3

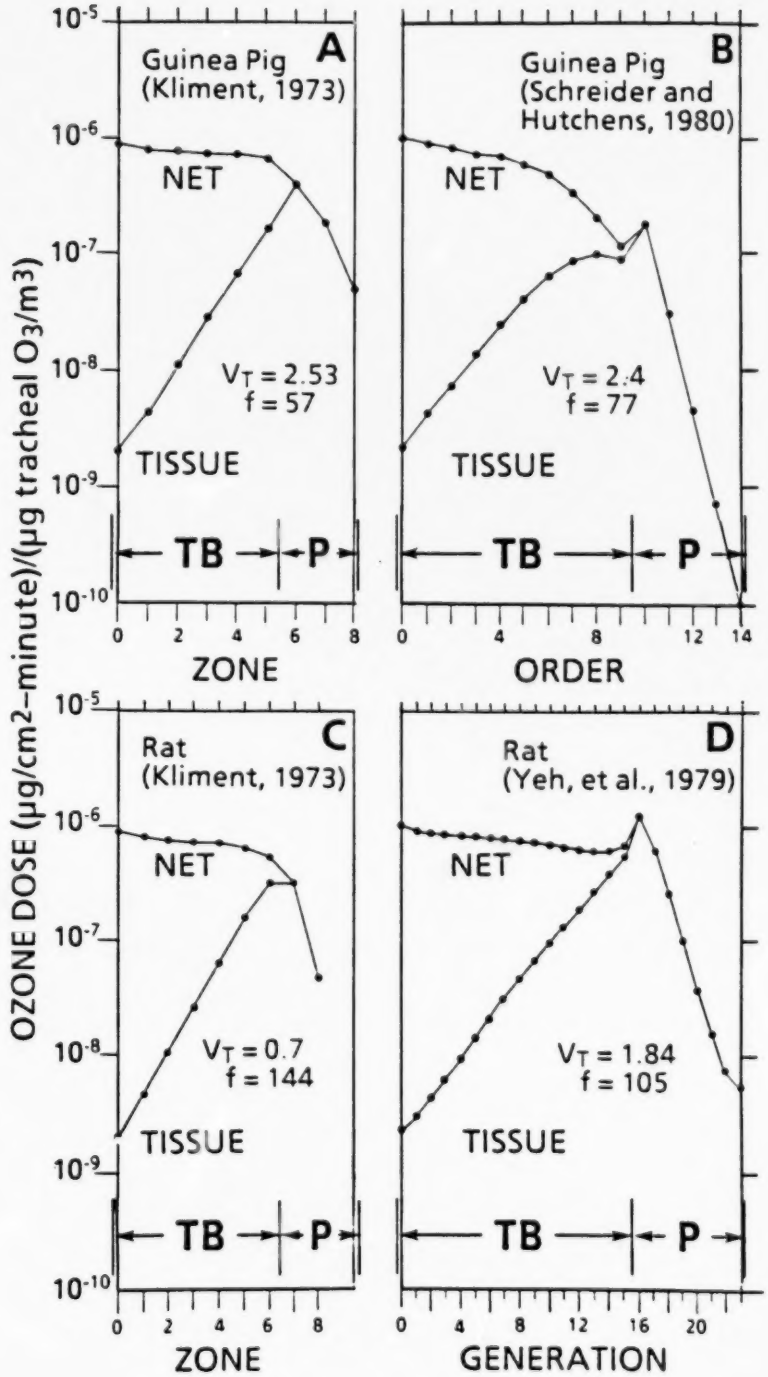
A
Guinea Pig
(Kliment, 1973)
NET
V_T = 2.53
f = 57
TISSUE
TB
P
ZONE
B
Guinea Pig
(Schreider and
Hutchens, 1980)
NET
V_T = 2.4
f = 77
TISSUE
TB
P
ORDER
C
Rat
(Kliment, 1973)
NET
V_T = 0.7
f = 144
TISSUE
TB
P
ZONE
D
Rat
(Yeh, et al., 1979)
NET
V_T = 1.84
f = 105
TISSUE
TB
P
GENERATION
OZONE DOSE (µg/cm²-minute)/(µg tracheal O₃/m³)

Fig. 4

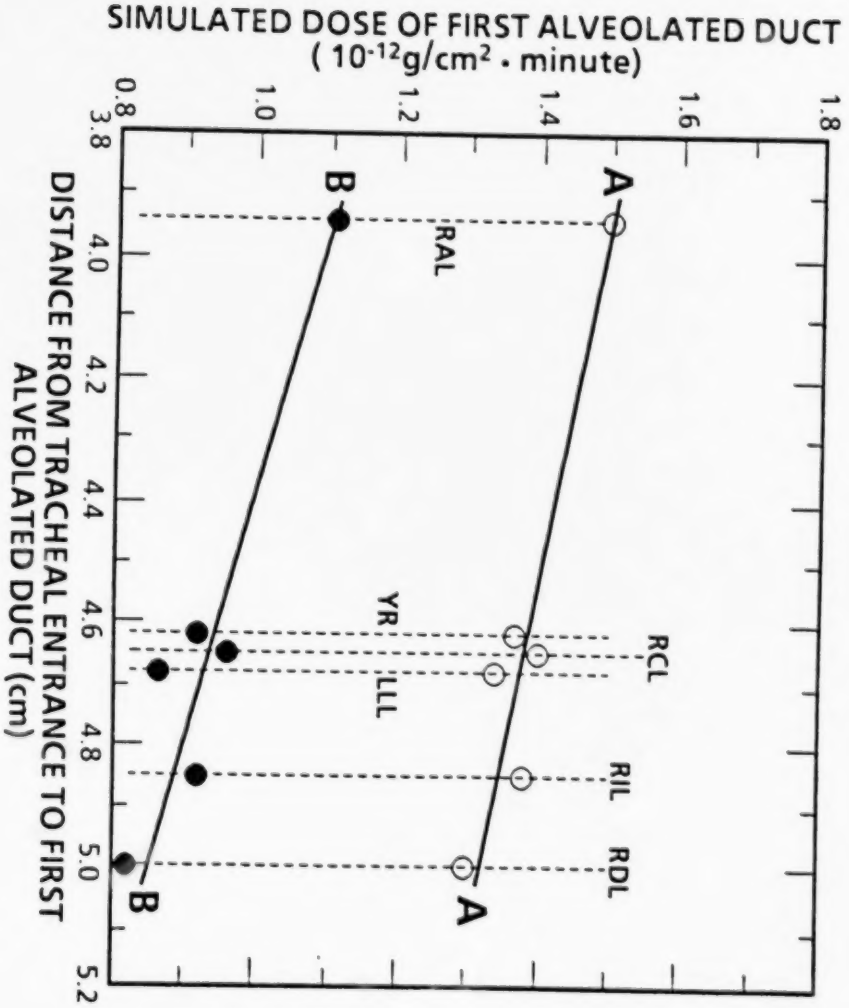
SIMULATED DOSE OF FIRST ALVEOLATED DUCT
(10-12g/cm2 • minute)
0.8
1.0
1.2
1.4
1.6
1.8
DISTANCE FROM TRACHEAL ENTRANCE TO FIRST ALVEOLATED DUCT (cm)
3.8
4.0
4.2
4.4
4.6
4.8
5.0
5.2
A
B
RAL
YR
LLL
RCL
RIL
RDL

Fig. 5

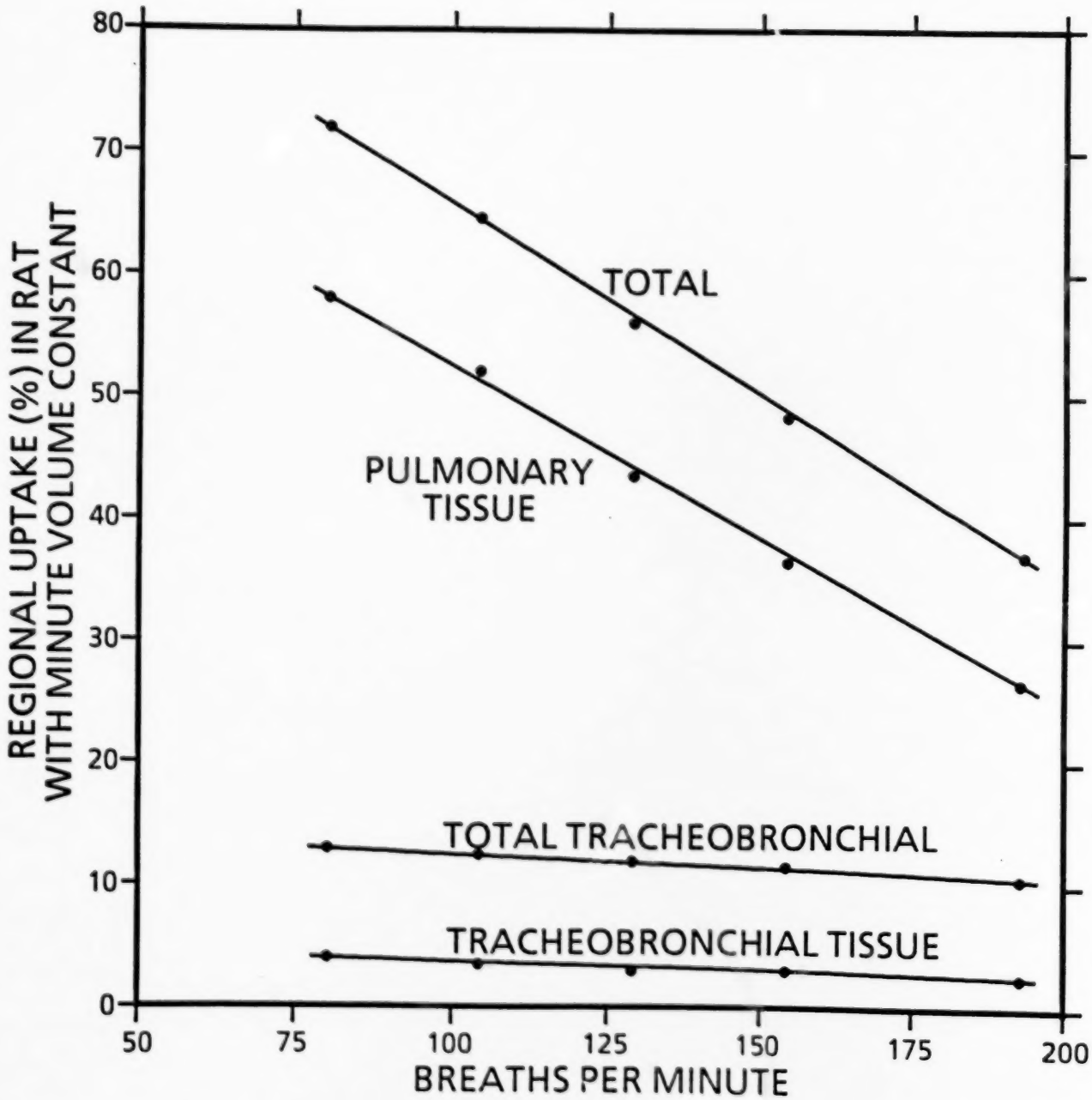
REGIONAL UPTAKE (%) IN RAT
WITH MINUTE VOLUME CONSTANT
80
70
60
50
40
30
20
10
0
TOTAL
PULMONARY
TISSUE
TOTAL TRACHEOBRONCHIAL
TRACHEOBRONCHIAL TISSUE
50
75
100
125
150
175
200
BREATHS PER MINUTE

Fig. 6A

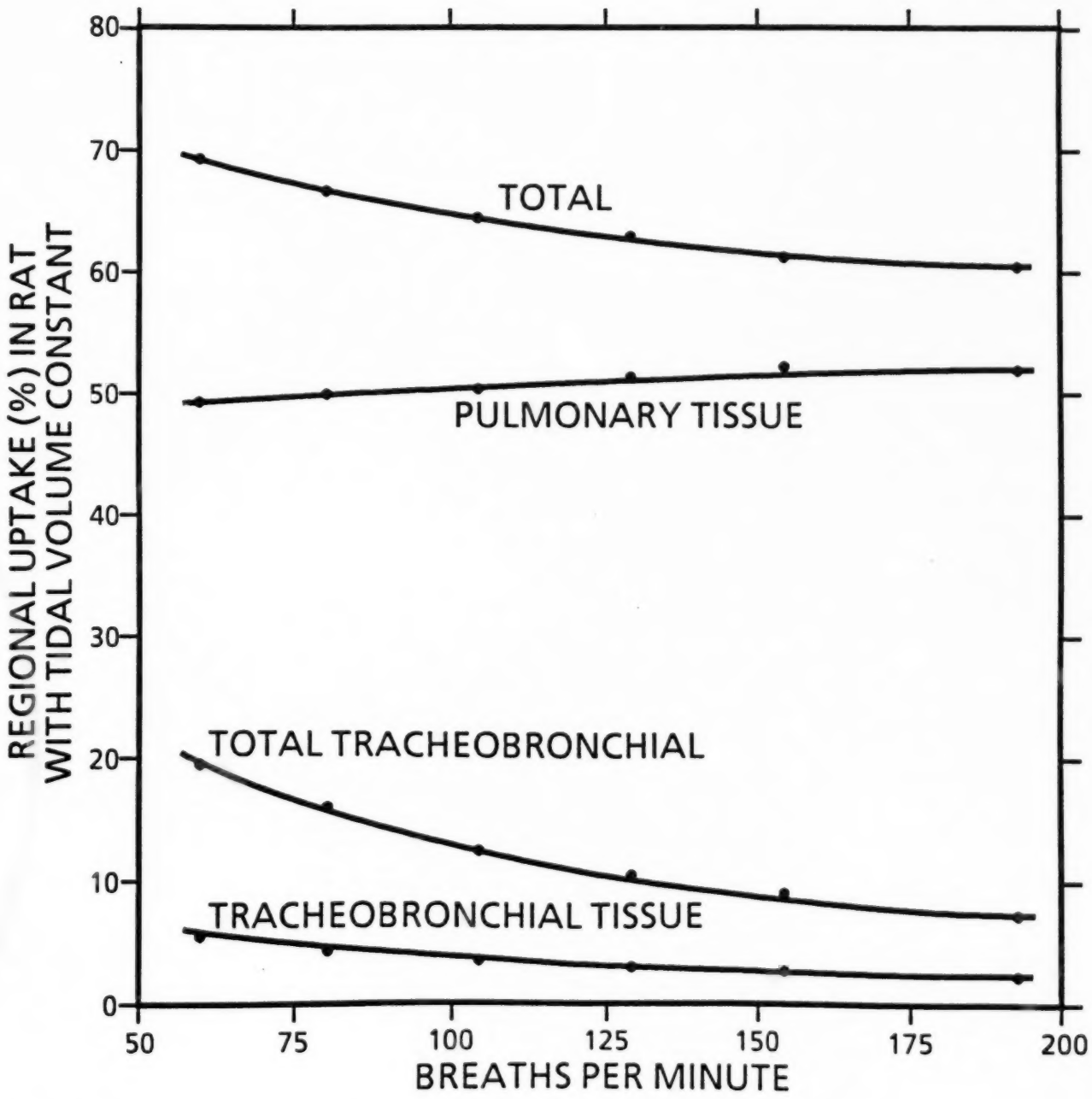
REGIONAL UPTAKE (%) IN RAT
WITH TIDAL VOLUME CONSTANT
80
70
60
50
40
30
20
10
0
TOTAL
PULMONARY TISSUE
TOTAL TRACHEOBRONCHIAL
TRACHEOBRONCHIAL TISSUE
50
75
100
125
150
175
200
BREATHS PER MINUTE

Fig. 6B

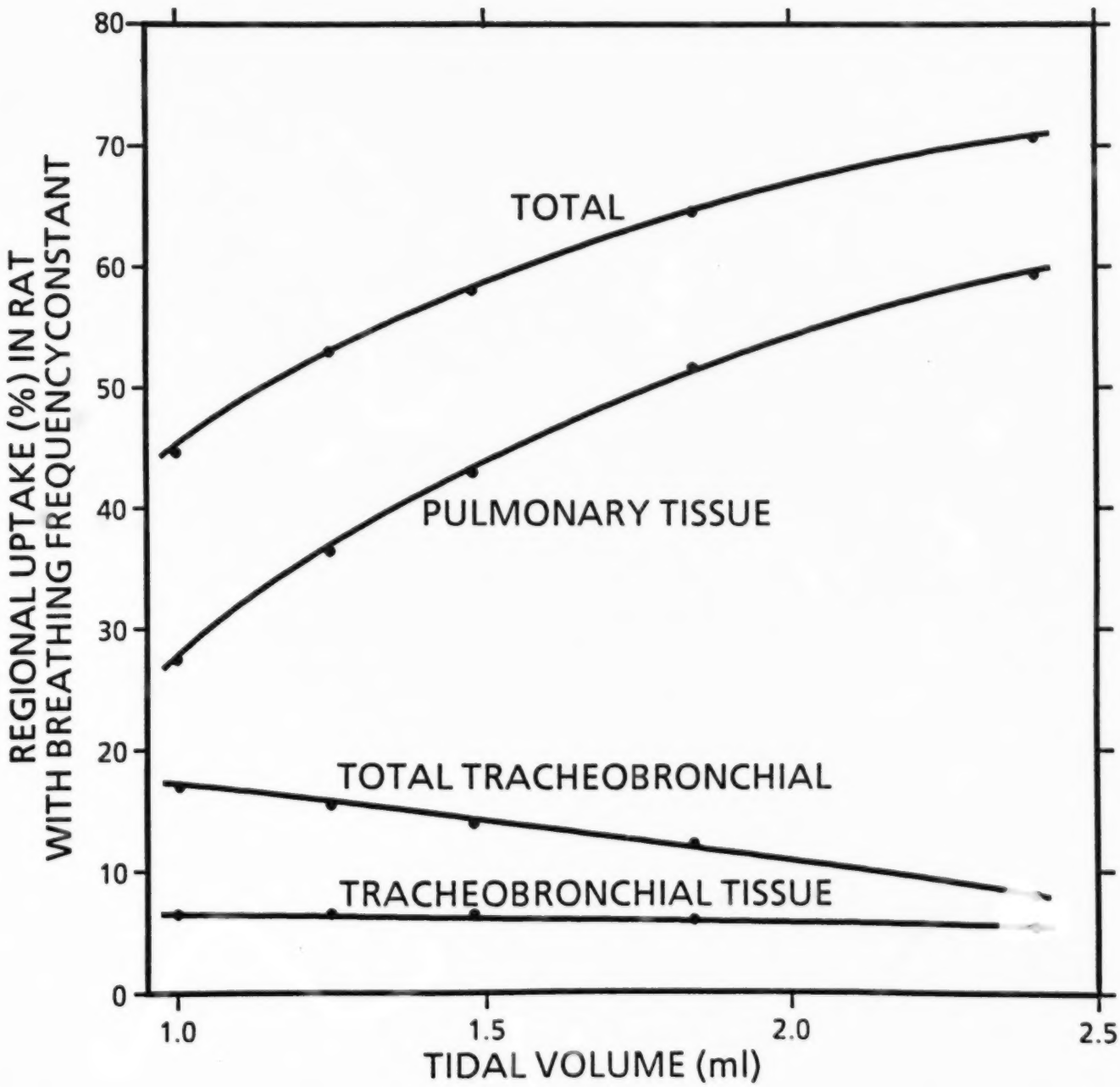
REGIONAL UPTAKE (%) IN RAT
WITH BREATHING FREQUENCY CONSTANT
80
70
60
50
40
30
20
10
0
TOTAL
PULMONARY TISSUE
TOTAL TRACHEOBRONCHIAL
TRACHEOBRONCHIAL TISSUE
1.0
1.5
2.0
2.5
TIDAL VOLUME (ml)

Fig. 6C

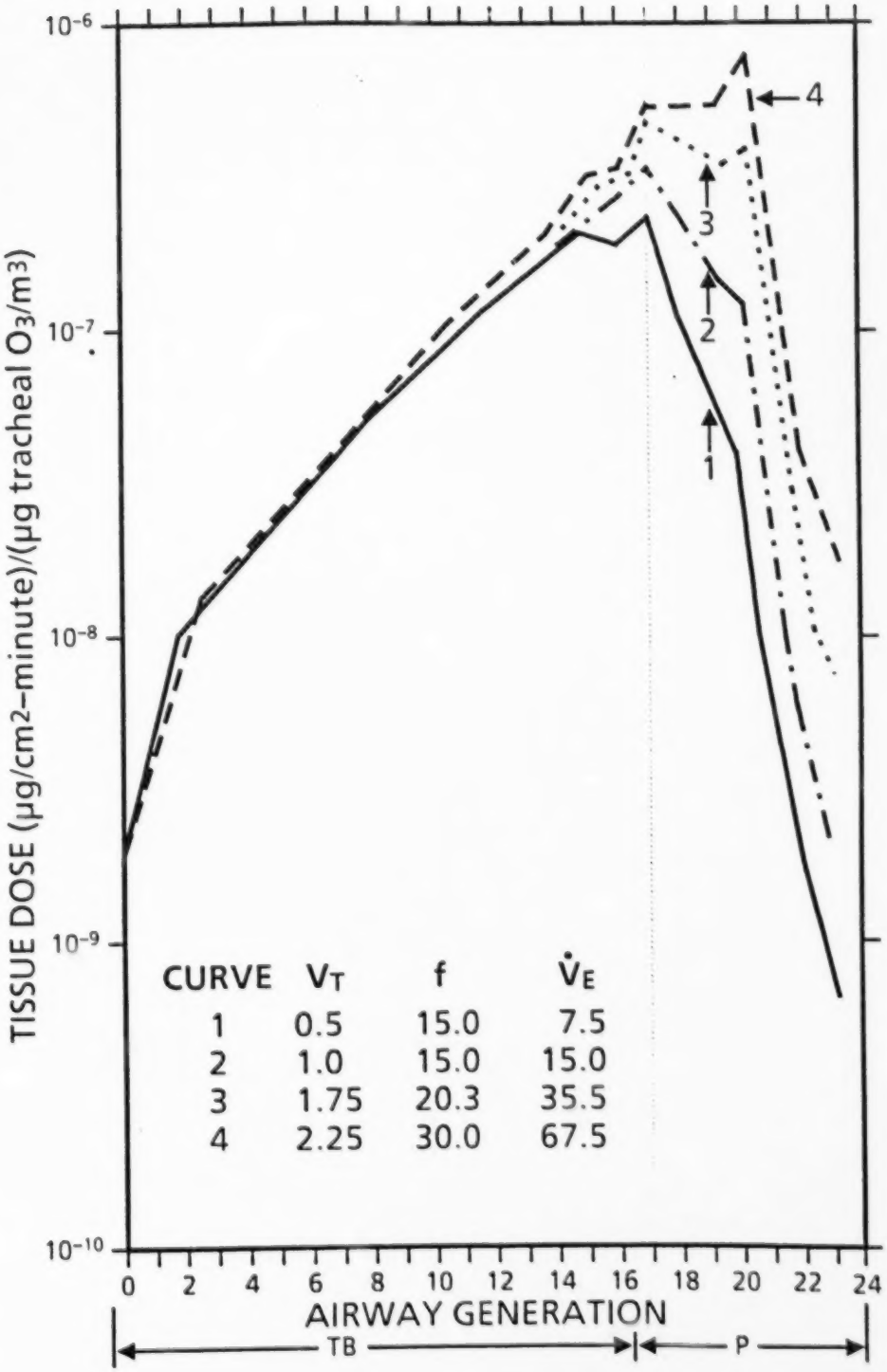
TISSUE DOSE (μg/cm²-minute)/(μg tracheal O₃/m³)
10⁻⁶
10⁻⁷
10⁻⁸
10⁻⁹
10⁻¹⁰
1
2
3
4
CURVE V_T f V̇_E
1 0.5 15.0 7.5
2 1.0 15.0 15.0
3 1.75 20.3 35.5
4 2.25 30.0 67.5
0 2 4 6 8 10 12 14 16 18 20 22 24
AIRWAY GENERATION
TB
P

Fig. 7

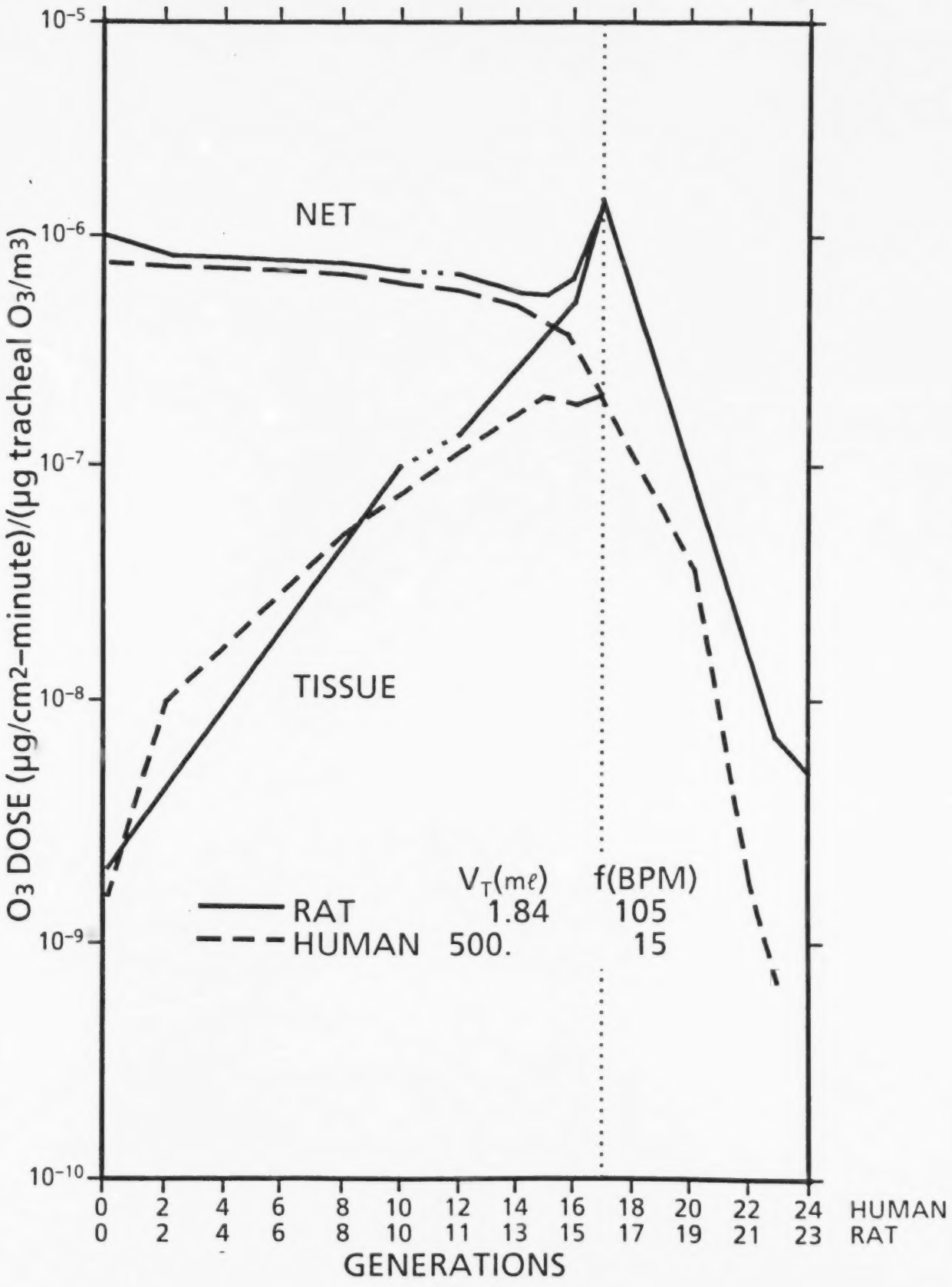
NET
TISSUE
O_3 DOSE (µg/cm²–minute)/(µg tracheal O_3/m³)
10^{-5}
10^{-6}
10^{-7}
10^{-8}
10^{-9}
10^{-10}
V_T(mℓ) f(BPM)
RAT 1.84 105
HUMAN 500. 15
0 2 4 6 8 10 12 14 16 18 20 22 24 HUMAN
0 2 4 6 8 10 11 13 15 17 19 21 23 RAT
GENERATIONS

Fig. 8